Korea-Australia Rheology Journal, Vol.26, No.3, pp.277-291 (August 2014) www.springer.com/13367
DOI: 10.1007/s13367-014-0032-2

# What are typical sources of error in rotational rheometry of polymer melts?

**Florian J. Stadler**[1,2,3,*]

[1]*College of Materials Science and Engineering, Shenzhen University, Shenzhen 518060, PR China*
[2]*Shenzhen Key Laboratory of Special Functional Materials, Shenzhen 518060, PR China*
[3]*Shenzhen Engineering Laboratory for Advanced Technology of Ceramics, Shenzhen 518060, PR China*

(Received April 1, 2014; final revision June 17, 2014; accepted July 9, 2014)

Rheometers have made giant leaps in terms of usability, sensitivity, and versatility. This leads to the illusion that a rheometer can be used as a fool-proof device for measuring rheological properties. The article will focus on typical problems that are encountered in rheological practice when measuring polymer melts. Emphasis is put on problems related to measurement artefacts stemming from the rheometer as well as from the material itself. Furthermore, possibilities to eliminate rheometer related artefacts mostly related to the following phenomena - geometry inertia, thermal expansion, torque resolution, and environmental control - will be discussed. The sample related artefacts vary significantly from sample to sample and include: thermal degradation, nonlinear shear deformation, centrifugal forces, slip and shear banding, as well as miscibility, orientation, and distribution of different phases, of which only the ones occurring in homogeneous polymer melts are discussed here.

***Keywords***: artefacts, inertia, thermal degradation, nonlinear regime, linearity and stationarity

## 1. Introduction

Rheology has gained significant attention in the last years due to its great utility in both modeling processing (Münstedt *et al*., 2005) and investigations of molecular structure (Dealy and Larson, 2006; Graessley, 2008). The development of modern rheometers has turned these complex machines into seemingly fool-proof easy-to-use machines, which, however, is a grave misjudgment. Scientific literature is filled with examples where rheological tests were performed but without really understanding the method of rheometry properly and, consequently, without removal of artefacts. In order not to libel anybody, only some of the author's data is discussed hereafter.

When performing rheological tests, a very common problem is to find proper conditions for measurement. Several factors need to be taken into account:

1) Torque resolution limit – given by the rheometer's sensitivity
2) Rheometer stiffness, especially geometry compliance
3) Inertia and its correction
4) Thermal expansion of the geometries (and also the sample itself)

Additionally, the material itself can also make some problems in getting proper data. Due to the limited amount of space for this article, only problems occurring in homogeneous polymer melts will be discussed:

1) Linear viscoelastic vs. nonlinear regime
2) Thermal stability
3) Stationarity in creep and oscillation
4) Wall slip and shear banding
5) Centrifugal forces

Other problems in measuring rheological data correctly not occurring in homogeneous polymer melts include

1) Solvent evaporation
2) Phase structure and its dependence on preshear conditions
3) Shear history
4) Orientation of non-symmetric fillers
5) Interactions between different components

This paper will give an overview of possible rheometer and polymer melt related artefacts. Each of the potential problems will be accompanied by an example from published and unpublished measurements, mostly by the author.

## 2. Encountered Artefacts

### 2.1. Rheometer related artefacts

#### 2.1.1. Choice of the geometry

The choice of the geometry influences the quality of the results. All samples with a *zero shear-rate viscosity* $\eta_0$ of more than 300 Pa s can be nicely rheologically characterized with a 25 mm parallel plate geometry, which is more or less the standard geometry used in rheology nowadays. When going to higher deformations or rubbery or even glassy samples, it is advantageous to use smaller geometries, typically parallel plate with a diameter of 8 mm.

Typically a gap of 1-2 mm is desirable. Smaller gaps than about 0.5 mm are very sensitive to imperfections of

# This paper is based on an invited lecture presented by the corresponding author at the 14th International Symposium on Applied Rheology (ISAR), held on May 22, 2014, Seoul.

*Corresponding author: fjstadler@szu.edu.cn

the plates, especially slight warpings of the geometry, which very easily happen, when, *e.g.* dropping a geometry accidentally or when using too much force when removing very stiff samples. Usually, such geometry imperfections lead to a too low modulus/viscosity, as slightly nonparallel plate-plate setups lead to gaps, larger than what is determined by the rheometer due to the fact that the zero gap is determined when the most protruding parts of a geometry touch each other. On the other hand, in continuous shear experiments, such warped geometries can also increase the viscosity, as the pure shear flow transforms to a combined shear and stirring flow, which contains additional elongational components. However, to the best knowledge, the effect of such geometry imperfections has not been studied so far.

For lower viscous fluids bigger parallel plate or cone and plate geometries should be used. Abovementioned issues of plate parallelism, obviously also apply for these to an even larger degree, as the higher weight of bigger plates and the larger size, while keeping the thickness approximately constant, means a higher susceptibility to plate deformation. In cone and plate geometries, the main problem that can happen is plate warpings, which leads to a stirring motion, but the set gap is correct usually, as the cone zeroing is done at the center of the geometry and not at an arbitrary position of the geometry, which protrudes most like a parallel plate geometry (obviously ideally, all positions of a parallel plate geometry should have the same distance from the other plate).

An alternative for low viscous materials is also the Couette or cup and bob geometry, which requires significantly more material for the measurement and is most often used for oils and other substances, which are fluids at room temperature. The general problem about this geometry is that sample loading is difficult, if the sample has either a high viscosity or is a solid at loading temperature, as the sample geometry effectively is a pipe closed on the lower end with very precisely defined thickness.

Hence, for high viscous materials, two problems are encountered. Firstly, loading a sample into a cup and bob geometry leads to significant orientations, which might take a very long time to relax. Using a vane, *e.g.* in cross-shape, simplifies the sample size somewhat but as a downside requires even more material and leads to a less defined flow field.

Another key point that needs to be taken into account is the symmetry of the geometry in the rotational axis, as otherwise sidewise motions of the fluid or in case of Couette geometries a stirring flow would be the consequence. Furthermore, the imbalance will lead to off-axis forces of the rheometer motor, which can distort the signal and worse in extreme cases destroy the air bearing. The latter is prevented by some rheometer models by limiting the rotational speed of Couette geometries.

#### 2.1.2. Influence of bubbles

Wolff and Münstedt (2013) showed that bubbles in the rheometer geometry lead to an increase of $G'$ at low $\omega$, sometimes by up to factor 10. Even small amounts of trapped air can lead to quite significant apparent increases in elasticity.

Such effects can even be observed for hydrophobic materials, as even for these, a small amount of $H_2O$ can be present adsorbed on the surface.

While this effect has certainly been encountered numerous times (*e.g.* Dijkstra, 2009) gave explicit advice about how to avoid it for Polyamide 6), it has only been investigated systematically by Wolff and Münstedt (2013) and, hence, the exact mechanism has not been revealed. While a lot of literature exists on the foaming behavior of polymers and soft matter (*e.g.* tensides and lipids), the gas content of these systems is always very high, typically more than 70% and, hence, these systems cannot be investigated by conventional rotational rheometers anymore.

It can be speculated that the trapped bubble is deformed elastically by the shear field. Due to the surface tension, the bubble is very elastic and, therefore, leads to an increase in elasticity.

This effect could be related to surface tension and is somewhat comparable to the additional relaxation process observed in polymer blends in the terminal regime (*e.g.* Friedrich and Antonov, 2007; Tao *et al*. 2013).

#### 2.1.3. Temperature calibration and thermal gradients

The temperature, a rheometer displays, is measured by a thermocouple or a resistivity device outside the sample, typically in one of the plates or close to the sample. Especially in test setups with non-constant temperature or with a large and poorly heat conductive sample, the question opens, as to how significant the difference between the sample temperature and the measured temperature is. The fact that the sample is usually significantly larger than for thermoanalysis (DSC – dynamic scanning calorimetry) limits, consequently, the maximum ramping temperatures to about ±5 K/min. However, due to the complex nature of thermal gradients and thermal conductivities in the setup and in the sample, it is not possible to give a general answer as to what is maximum temperature can be used. Furthermore, as gradients usually decay exponentially, it depends on the user's definition of which gradient is acceptable for the experiment to be conducted, *i.e*. the user can say that a temperature difference of 1 K is good enough or require a precision of 0.1 K. Obviously, reaching a temperature within ±1 K is significantly faster than ±0.1 K and, hence, the required waiting time before the experiment decreases.

Another source of error is that temperature sensors can change their characteristics with time, *e.g.* by oxidation or strong bending of cables. Hence, regular checks of the

temperature sensors is essential for keeping a measured temperature constant over a period of years and between different devices. Obviously, regular checks should be performed for all aspects of the rheometer *e.g.* for the deformation, normal force, and torque sensors, as well.

The effect of temperature on the rheological properties depends to a large extent on the type of sample used. For example, polyethylene is known to have an activation energy around 26-28 kJ/mol, while polystyrene has a WLF-temperature dependence (Williams *et al*., 1955), which corresponds to a temperature sensitivity around 150°C, which is about 30 times stronger than polyethylene's (Ngai and Plazek, 2007). In fact, a polystyrene with well-known rheological properties can be used as a very suitable material to check temperature and torque calibration of a rheometer, regularly.

Hence, the acceptable temperature error depends significantly not only on the accepted uncertainty in temperature but also on the material used.

#### 2.1.4. Thermal expansion of the geometry

Modern rheometer software has the possibility to compensate for the thermal expansion of the geometry by entering either a precalibrated thermal expansion value or to determine the thermal expansion by a measurement protocol. Anton Paar has the TruGap®-option, which overcomes these limitations by measuring the gap online, which, however, is not possible for all samples, as some fillers can disturb the measurement of the gap. While, in general, these methods work reasonably well for most applications, thermal expansion can still cause problems for a variety of reasons.

1) Most software packages allow the thermal expansion to be either switched on or off. The consequence obviously is that it is easily possible to use incorrect settings.
2) The thermal expansion coefficient $\alpha$, typically in the range of 1-3 μm/K, depends on a variety of factors:
   a) The material of the geometry: while in most cases stainless steel geometries are used, some special applications demand use of *e.g.* Al or high performance polymer geometries, which have significantly higher thermal expansion coefficients, which depending on the software might have to be adjusted manually or to be measured and registered with the geometry, which is easily forgotten.
   b) The environmental controller: depending on the size and type of the oven (and also depending on the material used for the geometry), a different temperature gradient is encountered, which is time dependent additionally. Hence, not only each geometry has its own thermal expansion coefficient, but it also depends on the size and type of the oven. For example, the same geometry will show a higher thermal expansion coefficient, if it is in an oven, which heats a longer section of it, as geometries made of poorly heat conductive materials such as stainless steel usually show a significant temperature gradient between the coupling connected to the usually cooled motor and the measuring end of the geometry.
   c) When changing the temperature, gradients exist in the environmental test chamber but also in the geometry, which take several minutes to get into equilibrium. Measurements performed before this thermal equilibrium has been achieved, unavoidably, will have a different measurement gap than the software records, which results in different rheological properties. This can be seen when setting the rheometer to push the plates together by a small normal force without sample in between and then measure the gap as a function of time (theoretically, it should be zero, of course) upon commanding a temperature change. Even in a very good oven, reaching a constant gap value takes significantly longer than the time for reaching a constant temperature according to the temperature sensor showing that getting the geometry in thermal equilibrium is a process, which takes significantly longer than to set a constant temperature at its tips. However, these changes are rather small (<20 μm) and only matter for very small gaps and, thus, for cone and plate geometries. That is one of the reasons that for a long time, it was seen as a general rule that cone and plate geometries can only be used under isothermal conditions.
   d) The thermal expansion coefficient also depends on the temperature difference between room temperature and the set temperature, as the temperature gradient is affected by this difference in a non-trivial fashion.
3) The possible error that can be made depends on the geometry

The shear rate $\dot{\gamma}$ (at the rim of the geometry $\dot{\gamma}_R$) - and obviously all quantities derived from it ($\eta$, $|\eta^*|$, $|G^*|$, G, …) scales with the reciprocal gap 1/H in a parallel plate geometry,

$$\dot{\gamma}_R = \dot{\gamma}(R) = \frac{R \cdot \Omega}{H} \tag{1}$$

with R - geometry radius, H - gap of the parallel plate geometry, $\Omega$ - rotational speed.

The possible error due to a gap error is shown in Fig. 1 and clearly demonstrates that the problem is the more serious the smaller the gap is in a parallel plate geometry. Obviously, that also means that when heating the oven beyond a certain limit and having a small gap, the sample gets squeezed out completely and the plates push against

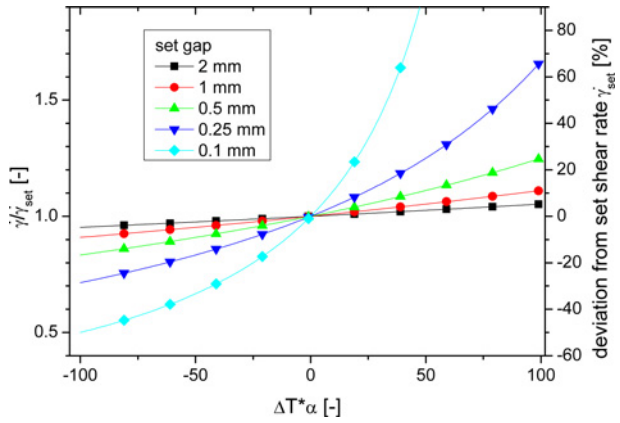


**Fig. 1.** (Color online) Possible error in shear rate due to thermal expansion coefficient mismatch for different set gaps.

each other, which could lead to catastrophically high normal forces and, consequently, to air bearing damage.

While it would be desirable to give the error in terms of viscosity or modulus, this is not possible in general. While the shear stress τ is independent of the gap in a parallel plate geometry, τ and consequently also the viscosity η depends on the shear rate $\dot{\gamma}$, unless a Newtonian material is measured. Hence, the error in viscosity depends on the shape of the viscosity function.

Furthermore, it is also obvious that cone and plate geometries are much more prone to such plate collisions, as the gap, *i.e.* the truncation of the cone, is usually significantly below 0.1 μm. Additionally, it is also clear that, while the geometry albeit with a different gap is still well-defined for a parallel plate geometry, a cone and plate geometry is strictly spoken only defined for one gap, which is given by the truncation of the cone.

### 2.1.5. Plate misalignment

After intensive use, quite often rheometer geometries are misaligned. In principle, there are two possibilities:

1) The plates are not completely parallel. This happens frequently when a geometry falls down – a rather common misfortune when cleaning it after a polymer melt. The consequence of this is that the gap is zeroed on the first point of contact. If part of the plate protrude a little, the gap will be underestimated, which leads to the same effect as a negative ΔT×α in Fig. 1. For cone and plate geometries, this error is usually less problematic, as the point of contact is well-defined anyway. However, in both cases the pure shear flow also gets a compressive/elongational component, which while having rather little effect on the viscosity, can significantly influence the normal force.
2) The axes are not aligned, *i.e.* the direction of the geometries' axes differs and/or the axes are not concentric. While the second type of offset is usually the consequence of poor setting up of the rheometer, the first one is usually done by careless users dropping the geometry or removing it from the fitting with too high force. However, it can also happen that an improperly set up rheometer has misaligned geometry mounts directionwise.

The consequences of warped geometries are underestimations of the gap due to the abovediscussed reasons and – worse – leads to an imbalance, which can damage the air bearing – particularly in tests involving fast rotations. Especially heavy bops are susceptible to this kind of problem.

If the misalignment is due to the geometry, it can be solved rather easily by placing the geometry in a milling machine and measuring the deviation while correcting the shape carefully with a rubber hammer. Worse warpings of the geometry surfaces can be corrected by milling off the surface of the geometry. Misalignments of the fittings themselves need to be corrected by a service engineer usually.

### 2.1.6. Too low torque

Fig. 2 shows the effect of reaching the torque limit on the TA ARES. The sample is a low viscous telechelic polybutadiene supramolecularly crosslinked with the weak ion butyl amine in the terminal regime, which can be seen from the terminal slope of $d\log G''(d\log\omega)=1$ for small ω (see black line in Fig. 2). It is obvious that for $\omega<2\ s^{-1}$ the rheological data starts looking strange. $\tan\delta$ increases significantly for $\omega=1\ s^{-1}$, then reaches a negative value for $\omega=0.46\ s^{-1}$ and $\omega=0.22\ s^{-1}$, which means $\delta>90°$.

Although the conditions were chosen to be suboptimal for the sample at this temperature (the aim of this test, being a subtest of a series, was to make a master curve from glassy to terminal regime), such problems can happen frequently, especially when measuring materials in the terminal regime with a strain-controlled rheometer. The general problem is to find conditions, under which a sample will give the information desired by the user.

The low torque limitation especially applies to strain controlled rheometers, measuring samples in the terminal regime, whilst staying in the linear viscoelastic range of deformation, as under normal circumstances, the deformation $\gamma_0$ is set to be constant, which means that $\tau\sim|G^*|$ and, hence, τ changes by up to a power law slope of 1.

Considering that the dynamic range of older rheometers is around 4 decades in torque, it is clear that in the terminal regime, it is often not always possible to use the same deformation in a frequency range of 3 decades or more. It is also not possible in most cases to start from the maximum torque and then go to the minimum value due to the desired deformation to be applied *e.g.* in the linear-viscoelastic regime.

As in stress controlled rheometers, often $\tau_0$ is set, this

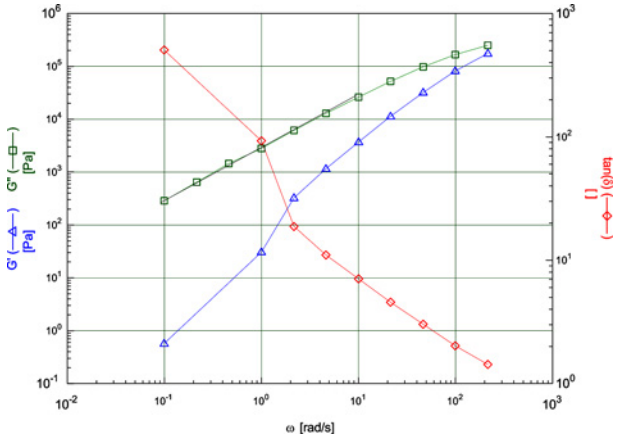


**Fig. 2.** (Color online) Incorrect measured data for a telechelic polybutadiene with a weak ion (butyl amine, Stadler *et al*., 2009), T = 10°C, $\gamma_0$ = 1%, 8 mm parallel plates, gap = 1.5 mm.

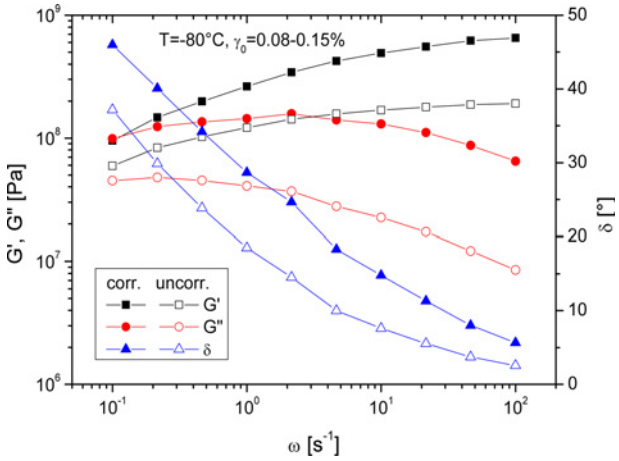


**Fig. 3.** (Color online) Frequency sweep of a telechelic polybutadiene with a strong ion ($Rb^+$) near the glass transition temperature (Stadler *et al*., 2009).

problem does not occur to the same extent for stress controlled test setups (unless the chosen torque $\tau_0$ is too low for the rheometer resolution for all frequencies). However, as will be shown later (Fig. 17), the consequence is that the linear viscoelastic regime might be exceeded and, hence, the data will be affected as well.

Some modern rheometry programs allow for programming strain adjustment routines, *e.g*. the TA Orchestrator has the AutoStrain function and Malvern's Gemini and rspace programs have different routines for adjusting the strain or deformation amplitude within one frequency sweep test. All of these functions have in common, however, that they are not purely automatized and require the user supplying enough data for a proper adjustment, which can only be done by experienced users knowing enough about the material to select proper parameters.

### 2.1.7. Geometry compliance

The topic was in detail discussed by Liu *et al.* (2011), who found that the problem is significantly more frequently encountered than believed in general.

Fig. 3 shows a frequency sweep of a material close to the glass transition using 8 mm plates and a gap around 1.36 mm. The open symbols are the measured data without the application of any correction routine, while the filled data were corrected according to the procedure described by Liu *et al.* (2011), which are significantly higher and less elastic than the measured data.

This is a general finding – samples beyond a certain stiffness appear to be less stiff than they are, as the effective deformation is lower than the applied deformation, due to geometry deformation as well. As a rule of thumb, it can be stated that for a normal parallel plate stainless steel geometry (1-2 mm gap), a geometry compliance correction becomes necessary above the following values for the complex modulus $|G^*|$: 8 mm, $|G^*| > 5\times10^7$ Pa; 25 mm, $|G^*| > 5\times10^5$ Pa; 40 mm, $|G^*| > 10^4$ Pa.

In general, the geometry compliance value can be looked up in the manual of the manufacturer or the data sheet of the geometry, but it is also possible to assess it from the shape of the data, when measured in the glassy regime. To do that two samples with significantly different thickness (*i.e*. different gap) should be measured. When executing the correction procedure the proper stiffness constant is found when the corrected data measured with both gaps agree.

The geometry compliance correction usually works well, as long as the correction factor is below factor 10 in $|G^*|$. As the sample stiffness scales with reciprocal gap 1/H and radius to the third power (in a parallel plate geometry), it is recommended to increase the gap and decrease the plate diameter when measuring very stiff samples.

### 2.1.8. Geometry and motor inertia

A typical geometry weighs 100 g and the moving parts of the motor weigh even more. Hence, it is not surprising that accelerating these parts requires some force, which can be very significant in comparison to the energy required for the sample deformation, if the viscosity of the sample is low or, in case of a dynamic-mechanical experiment, if the frequency is high. Electrical engineering has developed several methods for minimizing these effects, and, hence, these sophisticated correction routines prevent inertial problems appearing more frequently. However, while prescribing a certain additional torque to a measurement system so that it accelerates faster to the desired shear rate $\dot{\gamma}$, doing the same in dynamic-mechanical experiments is significantly more complicated. The simple reason is that here also the phase angle information has to

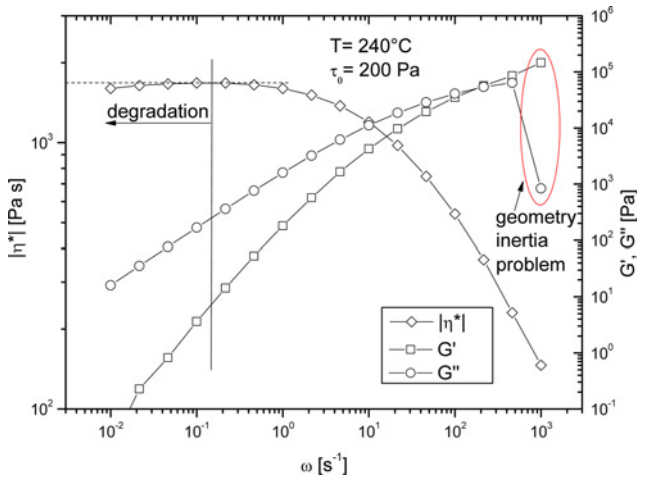


**Fig. 4.** (Color online) Frequency sweep of a commercial syndiotactic PP.

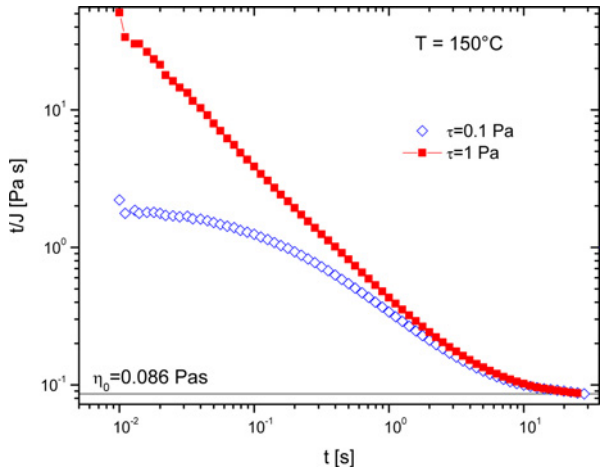


**Fig. 5.** (Color online) Creep test of low molecular mHDPE E7 with two different shear stresses.

be corrected for and typically, the phase angle $\delta$ shows incorrect values significantly before any problems are encountered in the modulus $|G^*|$. An example for an incorrect phase angle is given in Fig. 4, also Fig. 17 contains a comparable result.

While in the case of start-up flows and dynamic-mechanical tests as well as for other strain controlled experiments, it is possible to make a correction, it is not possible to do so for creep tests, as the deformation vs. time is not only dependent on the applied stress but also on the material behavior. Hence, finding a cogent way to correct for such problems is impossible.

Fig. 5 shows a creep test of a low molecular mHDPE (Stadler *et al*., 2006c), which should be a Newtonian liquid based on the low molar mass not allowing for more than 3 entanglements per chain, which according to established scaling last should relax in the sub-millisecond range. However, the data in Fig. 5 show that the viscosity sets off at significantly higher "viscosity" $t/J$ (actually, the quantity is creep time divided by creep compliance, but the quantity resembles the viscosity function as a function of $1/\omega$ or $1/\dot{\gamma}$ well) and then continuously decreases until reacting $\eta_0$ after about 20 s.

This decrease of t/J is related to the inertia of geometry and motor. This problem, obviously can be solved easily by increasing the creep time and it mainly occurs for materials, which are as low in viscosity as the one shown in Fig. 5. Hence, the inertia in creep tests shows up but extending the experimental time can solve the problem satisfactorily. Another way in modern rheometers is to set a constant shear rate and measure as a function of time. That way the sophisticated correction routines for inertia can be used and a constant Newtonian viscosity is reached faster for Newtonian or almost Newtonian samples.

One way to overcome inertia effects for strain-controlled experiments is to use a setup where motor and force transducer are located on opposite sides of the plate. The advantage is clearly that the torque measuring plate, in this case, is not moving and, hence, no inertia has to be overcome. Currently, two rheometer models are on the market with this configuration – TA Instruments ARES-G2 (and its previous versions) and Paar MCR 702. While this separate motor and transducer setup has big advantages, it increases the costs significantly, as one motor and one transducer or two motor/tranducer combinations have to be built separately, which makes the rheometer about 50% more expensive than a combined motor and transducer rheometer with otherwise comparable properties.

#### 2.1.9. Residual torque and creep recovery tests

The exact determination of the elastic compliance requires a bearing free of any parasitic moment or residual torque, which, of course, does not exist. Every existing bearing has some degree of parasitic force remaining even after applying sophisticated corrections such as the so-called '*torque-mapping*' used by modern rheometers which adjusts the motor (at each rotational angle) to apply a stress to counter the effects of the air bearing drift as much as possible (Barnes and Bell, 2003). Even after this correction a small amount of parasitic moment still causes a drift.

The drift caused by the parasitic moment is assumed to be time-independent. Thus, the elastic compliance can be corrected by introducing a correction constant $C$ according to

$$J_r(t) = J_r^{uncorr}(t) - C \cdot t \tag{2}$$

determined from the constant slope at long measurement times (typically $t > 2 \times t_0$) of $J_r(t)$ in linear scaling (Gabriel

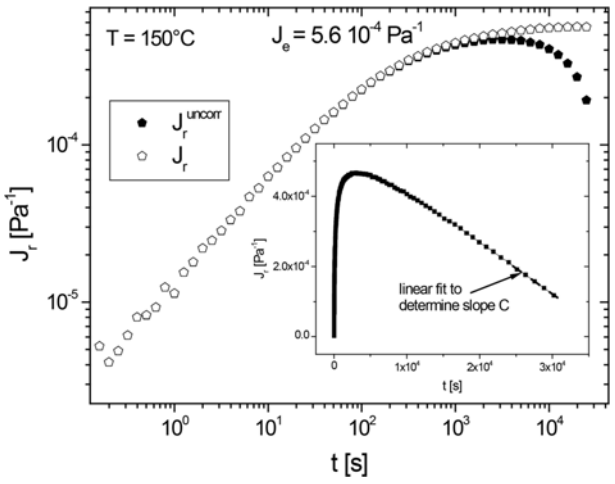


**Fig. 6.** Example of a drift correction (sample LCB-mLLDPE F12B); filled symbols – uncorrected $J_r^{uncorr}(t)$, open symbols – drift corrected $J_r(t)$. The small figure shows the linear plot with the fit determined used to determine the drift correction constant C.

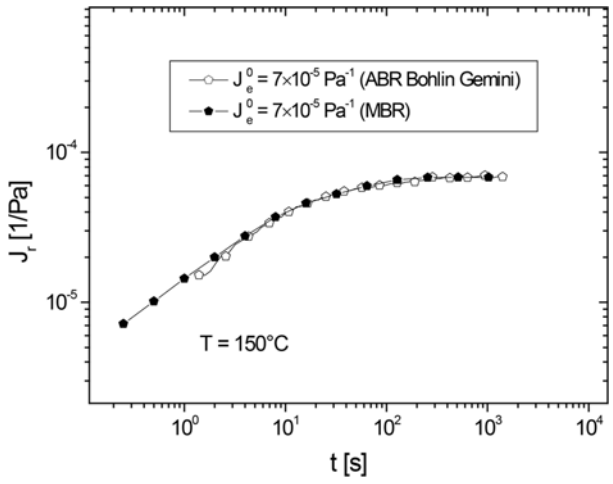


**Fig. 7.** Comparison of $J_r(t)$(corrected) of mLLDPE L4 (Stadler and Münstedt (2008)), the MBR data is taken from Gabriel (2001) (mLLDPE 1, same material and same batch as L4).

and Kaschta, 1998). An example for the drift correction is shown in Fig. 6. The material F12B is a ethene-/dodecene-copolymer with a very low degree of *long-chain branching* and a molar mass $M_w$ of around 170 kg/mol (Stadler *et al*., 2006b).

The parasitic stress $\tau_{drift}$ of the bearing can be calculated from the drift constant as

$$\tau_{drift} = C \cdot \eta_0 \cdot \tau \tag{3}$$

where $\tau$ is the stress of the preceding creep test and $\eta_0$ is the *zero shear-rate viscosity*. The parasitic moment can be calculated from $\tau_{drift}$ by applying the equations for the used geometry.

Gabriel and Kaschta (1998) compared the magnetic bearing rheometer (*MBR*) (Plazek, 1968), a rheometer constructed by Link and Schwarzl (1985) to the air bearing rheometer *Bohlin CSM*. Gabriel and Kaschta (1998) stated that the main disadvantages of the air bearing rheometers are the high friction due to the extremely small gap for the air flow centering the bearing (leading to a lower $J_r(t)$), higher inertia of the rotor (resulting in a worse short time resolution), a worse spatial resolution, and a higher parasitic moment.

However, comparisons between data published by Gabriel (2001) for the *MBR* and measurements on the newer air bearing rheometer (ABR) Rheometer Bohlin CVOR "*Gemini*" (Fig. 7) showed an excellent agreement in the elastic compliance $J_r(t)$ for *mLLDPE* L4 (Stadler and Münstedt, 2008) - only the short time regime is resolved better by the *MBR* (Gabriel, 2001).

Edler (1986) determined the parasitic moment of the *MBR* to be $3\times10^{-8}$ Nm. Measurements of the parasitic moment of the *Gemini* yielded the same value on the average; however, this value is changing distinctly from one measurement to the next one. The explanation is that the rotational position of the creep recovery measurement (due to the very small movement, we can assume that the bearing position stays constant enough to not affect the residual torque) is different for every experiment. Thus, the drift constant is different for each measurement with the *Gemini*. For some measurements it was possible to determine drift free creep recovery data with the *Gemini*.

This indicates that two of the disadvantages of the air bearing stated by Gabriel and Kaschta (1998) – the high friction and the high parasitic moment – are not applicable to state-of-the-art air bearing rheometers anymore. Highly precise measurements of the short term elastic compliance with the *MBR* are also very complicated.

## 2.2. Material related artefacts

This section deals with the artefacts caused by the material that are encountered when measuring homogeneous polymer melts only. Artefacts specific to blends, composites, gels, emulsions, suspensions, and solutions will not be covered in this article.

### 2.2.1. Stationarity in oscillatory measurements

The question how many periods of oscillation are required for the stationarity in oscillatory measurements is an important point, as all the definitions for the oscillatory measurements are only valid for steady-state oscillatory measurements, *i.e*. theoretically for an infinite number of oscillations. Obviously, it is not possible to perform a test to infinite time for every condition, *i.e*. every frequency $\omega$ and every deformation $\gamma_0$. Thus, the question persists how many oscillations are required to

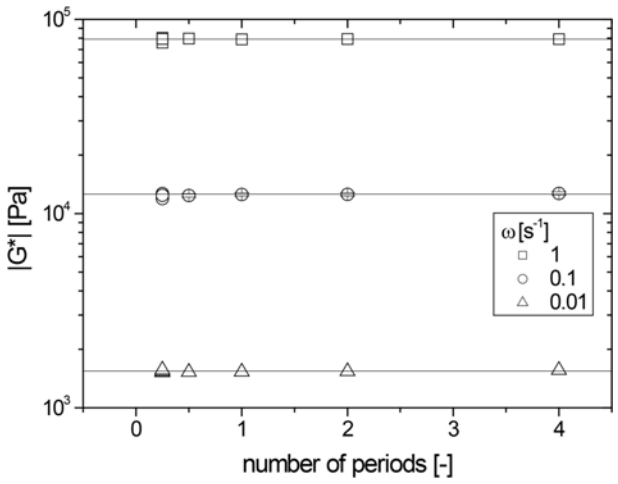


**Fig. 8.** Change of the complex modulus |G*| of mLLDPE F26F (Stadler and Münstedt (2008)) at a different number of oscillation periods. The error bar (only shown for $\omega$ = 0.1 $s^{-1}$) is ±2%, the reproducibility of an oscillatory test with the same sample.

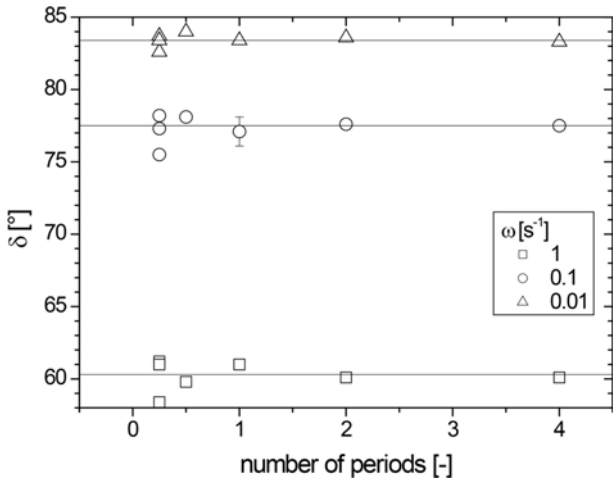


**Fig. 9.** Change of the phase angle d of mLLDPE F26F at a different number of oscillation periods. The error bar is equivalent to ±0.7°, the reproducibility of an oscillatory test with the same sample under the same conditions.

reach the steady state.

In the case of high frequencies, the number of periods taken for the acquisition of the data point does not play such a dominant role as the periods are very short, but for very low frequencies, this is a crucial question, as a reduction of the number of periods used for the data point accounts for a significant reduction of the measurement time, *e.g.* at a frequency $\omega$ of 0.01 $s^{-1}$ a measurement time of 628 s (10.5 *minutes*) per period is required.

For this reason, oscillatory tests were carried out with a different number of periods on the same sample and subsequently compared. The complex modulus (Fig. 8) stays the same for the measurements conducted with 0.5, 1, 2, and 4 periods within an error of ±2%. Thus, it can be concluded that the evaluation of half a period is sufficient for the determination of the complex modulus $|G^*|$, which is calculated from the ratio of the stress and the deformation.

The phase angle $\delta$, however, is much more sensitive to an insufficient number of oscillations which is evident from Fig. 9. The error bar in this figure is equivalent to an experimental uncertainty of ±0.7° which is the reproducibility in a repetition of the test.

The conclusion is that 1 period is required for the acquisition of correct values of the phase angle $\delta$. There is no systematic deviation between 1 and 4 periods, which means that the scattering is statistical. Therefore, for most materials as a standard, oscillatory tests should be carried out using one period.

It should be mentioned that in large amplitude oscillatory shear, where the raw data is analyzed, usually at least 1 full oscillation has to be performed before the material is in equilibrium conditions (Wilhelm, 2002), as can be seen from Fig. 10. Material 1 (thin black line) shows a fast transition to equilibrium, while material 2 (shear stress τ multiplied by factor 50 for sake of clarity), which is of very similar composition, requires 8 cycles until having reached equilibrium. Both tests were performed with an identical test setup (ARES, 50 mm 0.02 rad cone and plate) and identical set conditions ($\omega$ = 1 $s^{-1}$, $\gamma_0$ = 1440%).

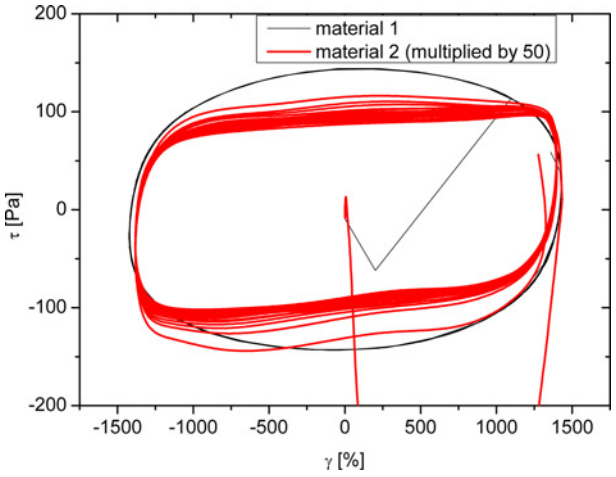


**Fig. 10.** (Color online) LAOS of two CNT-containing polymer solutions with significantly different properties.

The conclusion is that even seemingly similar materials can have a significant difference in terms of periods required to reach equilibrium under nonlinear oscillatory testing, which obviously needs to be checked for performing reliable rheological tests.

### 2.2.2. Stationarity in creep recovery

In case of creep recovery tests, the linearity and the stationarity have to be proven. An extensive study on this has been published by Gabriel and Münstedt (1999) and by Wolff *et al*. (2010). Therefore, the approximate conditions for reaching the stationarity and linearity can be estimated from these experiments.

As a rule of thumb the deformation should not significantly exceed $\gamma = 1$ for polymer melts, which means that $t_0$ should be larger than $1/\dot{\gamma}$ ($t_0$). Hence, the creep stress $\tau_0$ should be set to below a value, which can be calculated from:

$$\tau_0 < \eta_0/t_0 \quad (6)$$

in general, it is better to use less than 50% of the value calculated from eq. 6, as in the beginning of the creep test, the shear rate $\dot{\gamma}$ is significantly higher than in the terminal regime. Obviously, it is not possible to know $\eta_0$ exactly before having performed a creep test and, thus, the zero shear-rate viscosity $\eta_0$ has to be guessed before the test, *e.g*. by extrapolating it from the dynamic-mechanical data.

An example of reaching the stationarity is plotted in Fig. 18 for the sample F26F, a linear *mLLDPE*. It is obvious that for a creep time of 100 s and a stress of 10 Pa the linearity and stationarity have not been fully reached, while this is the case for the longer preceding creep time of 10000 s at 10 Pa as $J_r(t, t_0 = 10{,}000$ s) and $J_r(t, t_0 = 20{,}000$ s) agree within the experimental error.

However, it also has to be taken into account that the elastic compliance is the least reproducible rheological quantity, as it is also the most demanding one to measure. For this reason the average reproducibility of $J_r(t)$ typically is in the order of ±5–15% instead of ±2–5% for $G'(\omega)$ and $G''(\omega)$ (for $\delta < 89^o$).

For proving that $J_e$ is $J_e^0$, the main limitation is the thermal stability of the samples, as these tests (measuring the stationarity requires creep measurements beyond the limit of stationarity, *i.e*. longer creep times than required) take a very long time. It also has to be considered that the drift effects increase with decreasing creep stress, as the ratio of the creep stress to the drift stress ($\tau/\tau_{drift}$) becomes smaller.

The effect of very large creep stresses on the creep recovery behavior is discussed in more detail by Patham and Jayaraman (2005), Münstedt (2014) and Wolff *et al*. (2010) leading to dramatic reductions of the recoverable compliance for large creep stresses ($\tau = 10000$–$30000$ *Pa*). This is reasonable, as the stationary value of the elastic compliance $J_r(t)$ in the non-linear regime is roughly equivalent to the linear elastic compliance at a time equivalent to the reciprocal stationary shear rate of the creep test $J_r^0(t = 1/\dot{\gamma})$ (Gabriel, 2001).

### 2.2.3. Thermal stability

2.2.3.1. Methods for testing thermal stability

It is a well-known fact, that most polymers require anti-oxidative stabilization. When intending to establish relationships between the molecular structure and the rheological behavior, it has to be assured that the former does not change during the test.

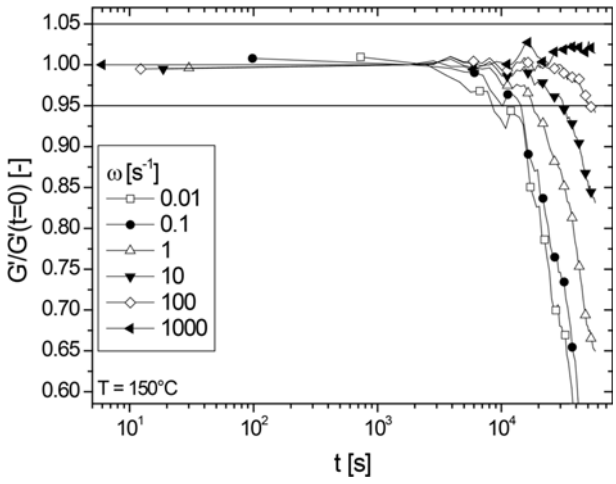


**Fig. 11.** Change of the storage modulus of LCB-mHDPE B11 for different frequencies.

As a standard a maximum deviation of ±5% from the initial value of the storage modulus $G'$ at the lowest frequency (mostly $\omega = 0.01\ s^{-1}$) should be adopted as the stability criterion. When the viscosity $|\eta^*(\omega = 0.01\ s^{-1})|$ is very close to the *zero shear-rate viscosity* $\eta_0$ (*i.e.* $\delta > 85°$) the determination of $G'$ might be no longer possible with sufficient precision due to the uncertainty in determining the phase angle $\delta$. In these cases the complex viscosity $|\eta^*(\omega)|$ can be employed, although this quantity is significantly less sensitive.

From the equations

$$G'(\omega \to 0) = \eta_0^2 \times J_e^0 \times \omega^2 \quad (4)$$

$$G''(\omega \to 0) = \eta_0/\omega \quad (5)$$

and the $\eta_0$-$M_w$-correlation ($\eta_0 \sim M_w^{3.4\text{-}3.6}$) it can be concluded that $G'(\omega)$ in the terminal regime is proportional to $\eta_0^2$ which means that $G'(\omega)$ is proportional to $M_w^{\approx 7}$ in the case of linear chains, while $G''(\omega)$ or $|\eta^*|(\omega)$ only scale with $M_w^{\approx 3.4\text{-}3.6}$.[†] Thus, the stability criterion ±5% is equivalent to a deviation in molar mass $M_w$ of ±0.6% when looking at $G'(\omega)$. This criterion is very strict in comparison to the resolution of the *SEC-MALLS* (≈±5%).

The sensitivity of the time sweep with respect to thermal degradation depends on the frequency (Fig. 11). The closer the frequency to the terminal regime the better is

[†] For *long-chain branch*ed and non-homogeneous samples (blends, composites, …) the change in the molecular structure when reaching a ±5% change in $G'(\omega)$ cannot be assessed as easily. Depending on the degradation mechanism even very small changes in molecular structure can already lead to dramatic changes in the rheological behavior.

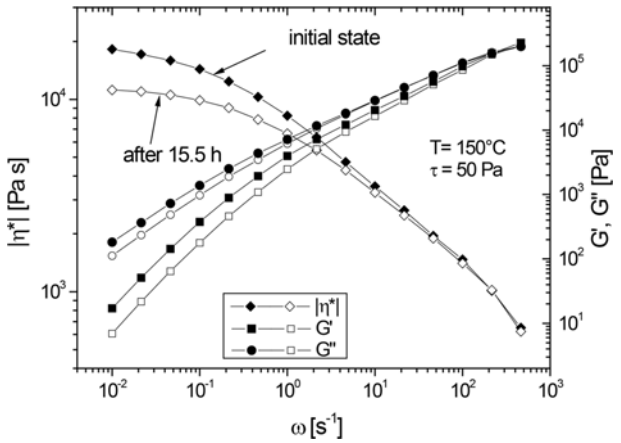


**Fig. 12.** Thermal degradation of LCB-mHDPE B11. The filled symbols refer to the initial state (t ≈ 0 h) while the open symbols stand for the state after the creep recovery test (t ≈ 15.5 h).

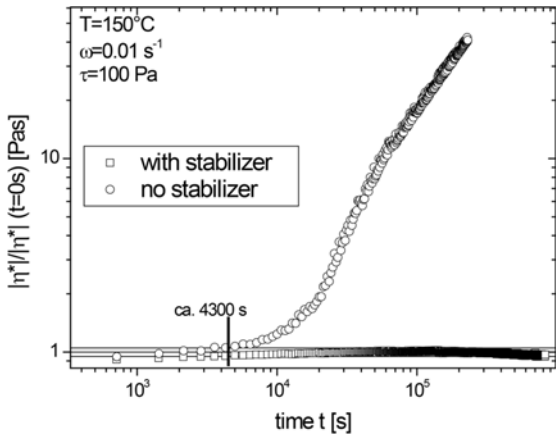


**Fig. 13.** Degradation of sample mLLDPE F18F. The unstabilized sample exceeds the ±5% criterion after 4300 s because of cross linking, while the stabilized sample stays within this criterion for 824,000 s (≈9.5 days).

the sensitivity of the test. This is shown exemplarily for B11 a slightly branched *LCB-mHDPE* with a *zero shear-rate viscosity* $\eta_0$ of 18,600 Pa s (Stadler and Karimkhani, 2011), which is not very much thermally stable. At $\omega = 0.01\ s^{-1}$, the viscosity $|\eta^*(\omega)|$ is 17700 Pa s, which means that this frequency is very close to the onset of the terminal regime ($\eta_0 = 18300 \pm 400$ Pas). For $\omega = 0.01\ s^{-1}$ and $\omega = 0.1\ s^{-1}$, a very distinct deviation from the ±5% criterion is found for measurement times exceeding approximately 10,000 s, while for high frequencies only a very small degradation is obvious. Hence, a measurement frequency chosen too high can lead to a grave overestimation of the thermal stability of the sample. On the other hand, it also means that when measuring from lowest to highest frequency for thermally unstable materials can extend the measurement time possible. However, this method bears the risk that even the first datapoint (the one with the lowest frequency is incorrect due to degradation.

A better approach is to violate abovementioned criterion for stationarity in oscillation and perform only half-waves on each sample and average 2 or more datasets. This will reduce the measurement time per sample and still allow getting good data, however, at the price of having to use at least twice as many samples as under normal conditions of reproducibility.

Fig. 4 shows the same phenomenon in a different way. A frequency sweep performed at a temperature close to the degradation temperature shows a decrease of $|\eta^*|(\omega)$ with decreasing $\omega$, which according to the linear viscoelastic theory is impossible and which was not observed for the lower temperatures. Hence, the sample degrades within the about 23 min of the experiment.

When characterizing a sample with a longer experiment, *e.g.* a long creep and creep recovery test an online quality check can be performed by applying a frequency sweep before and after the creep recovery test and afterwards checking for any degradation, which might have taken place during the long creep recovery test, by comparing the test before and after the long test. With this method it is only possible to perform a check but it is the assurance that the sample was stable during the whole test.

An example of this method is given in Fig. 12 for the *LCB-mHDPE* B11, which shows that this sample is not sufficiently stable to perform a creep recovery test lasting for 15 h.

2.2.3.2. Effectiveness of stabilization

The example shown (Fig. 13) illustrates the need for a proper stabilization as the unstabilized sample is starting to crosslink and, thus, exceeds the ±5% criterion (change in the rheological properties) after approximately $t_s$ = 4300 s (time of stability) because of crosslinking, while the stabilized sample only shows the onset of a decomposition after 9.5 days (≈830000 s)[‡]. In this case the complex viscosity $|\eta^*(\omega)|$ instead of the storage modulus was chosen as the scattering of the storage modulus was very large, due to the high value of $\delta$ leading to a scattering $\Delta G'$ of ±15%. This uncertainty is equivalent to $\Delta\delta \approx 0.5^{\circ}$.

The sample F18F is a linear *mLLDPE* with approximately 3 mol% of octadecene with a *zero shear-rate viscosity* $\eta_0$ of 145,800 Pa s (Stadler *et al*., 2007).

When characterizing unstabilized samples, in general, it is recommended to add an appropriate amount of stabilizer. The author has found that a stabilization of 0.5 wt.% Irganox 1010®, 0.5 wt.% Irgafos 38® or 168® works quite

[‡] The sample is still within the ±5% criterion after this long time and, when visually extrapolating the data, the time of stability $t_s$ is between approximately 11 and 15 days.

well for polyethylenes. The stabilizer can be added by mixing the pellets or powered polymer with the stabilized powder and shaking it thoroughly for several minutes in an inflated plastic bag or plastic bottle, which connects both components by static charges.

This amount is about 5 times higher than the amount used for industrial processing, but the rheological tests also take significantly longer.

2.2.3.3. Dependence of the thermal stability on synthesis conditions

At first glance there seems to be no reason for a dependence of the thermal stability on the synthesis conditions. However, as stated before *LDPE* does not require a thermal stabilization while conventional *ZN-PE* and *mPE* do (basell Polyolefins, 2003; den Doelder, 2004; Gabriel, 2001). This means that there has to be a fundamental difference in the chemical structure which causes this dissimilar behavior.

Fig. 14 shows that samples synthesized with *catalysts* A and B (Piel *et al*., 2006a) are not very stable ($t_s$≈10,000 to 20,000 s) while the samples synthesized with *catalyst* F have a higher thermal stability ($t_s$ > 80,000 s, Piel *et al*., 2006a; Stadler *et al*., 2006a). This means that *catalyst* F produces samples which are less susceptible to degradation or more in general that samples of very similar composition might have significant differences in terms of thermal stability.

A comparison between the samples synthesized with *catalyst* B (B9, B10, B11, Piel *et al*., 2006a) and the samples synthesized with *catalyst* F (Stadler *et al*., 2006a) by *NMR* showed that the former have several peaks pointing to groups containing oxygen (hydroxyl, acid, aldehyde, ketone, peroxide, …). These peaks were not found for the much more stable samples synthesized with *catalyst* F (Klimke, 2006). Hence, samples synthesized with *catalyst* B contain chain irregularities (of unknown chemical nature), which are oxidized after the synthesis Kaminsky (2004), Piel (2004). The concentration of these errors in samples synthesized with *catalyst* F is much lower in comparison. Hence, the *catalyst* F is producing *PE*-chains with a much higher perfection than *catalysts* B and A.

Another interesting finding is that the samples synthesized with *catalyst* F show a distinctly different time of stability $t_s$. The sample F0 with no comonomer and the highest degree of *long-chain branching* is only stable for one day, while the sample F12B with 1.5 mol% comonomer and a smaller degree of branching fulfills the stability criterion for two days and the linear sample F18F with 3 mol% comonomer does not violate the ±5% criterion for 9.5 days (830000 s).

Thus, either the comonomer itself is responsible for the increase in thermal stability or the reduced *long-chain branch* concentration being a consequence of the comonomer incorporation (see Karimkhani *et al*., 2013). The comonomer decreases the local mobility of a chain because of steric effects. Thus a radicalic chain end cannot move away from its original position to react with a neighboring chain as easily as a homopolymer chain. The other possibility is that a slight reduction of the *long-chain branch* concentration has a very distinct effect on the rheological properties and that a reduction of the *long-chain branch* length causes these distinct differences.[§]

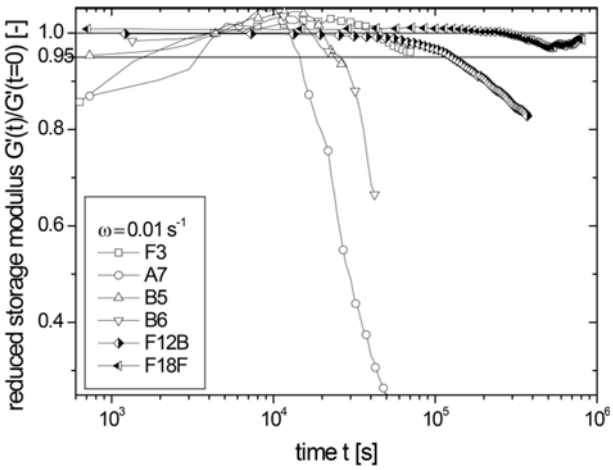


**Fig. 14.** Thermal stability of several linear, short-, and long-chain branched mPE samples synthesized with different catalysts under various synthesis conditions (see Piel *et al*., 2006a, 2006b) for exact synthesis conditions).

It also has to be considered that non-terminal vinyl groups, which are formed when a chain is terminated after the insertion of a longer comonomer, are sterically very hindered, which is also the reason why the direct synthesis (*i.e*. without any further additive or treating mechanism)[**] of branched *PP* has not been achieved yet (Kaminsky, 2004). It is obvious that a longer *a*-olefin has a stronger hindrance effect than the short propene.

2.2.3.4. Influence of oxygen and water

As all polymers are either completely organic or – in the case of silicones – contain organic side groups, oxidation is an effect that has to be taken into consideration and avoided unless the study aims to directly investigate the effect of oxidation.

Fig. 15 shows time sweeps of a commercial PP for film

[§] McLeish *et al*. (1999) and Frischknecht *et al*. (2002) stated for example that even minute changes (due to polydispersity) in the arm length of almost monodisperse H-polymers and asymmetric stars have a distinct effect on the rheological behavior.

**The methods for creating *LCB-PP* are peroxidative degradation (Auhl, 2006) *β*- or *γ*-irradiation (Auhl, 2006) copolymerization with *α*-,*ω*-dienes (Walter *et al*., 2001), copolymerization with vinyl chloride (Stadler *et al*., 2010), the chlorine is not included in the polymer chain) or the copolymerization of macromers and propene (Rulhoff and Kaminsky, 2006).

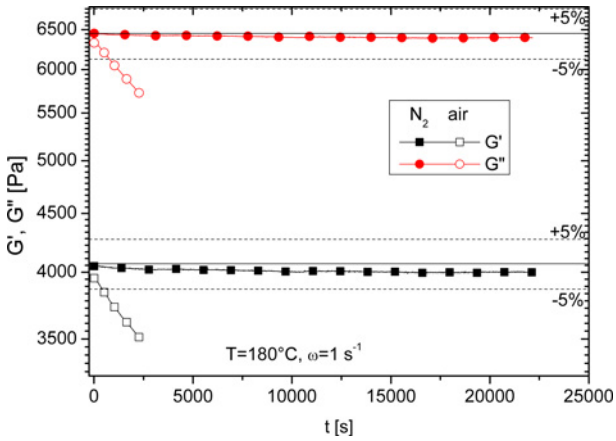


**Fig. 15.** (Color online) Thermal stability of a commercial polypropylene in air and $N_2$-atmosphere at 180°C.

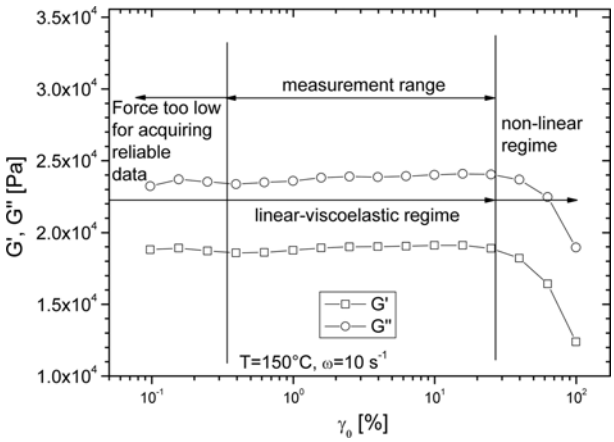


**Fig. 16.** Amplitude sweep of LCB-mHDPE B7. $\Gamma_0$ $\gamma_0$

applications under identical test conditions but the open symbols were measured in air atmosphere, while the filled symbols were measured in nitrogen, stemming from evaporated liquid nitrogen. It is obvious that the change of the rheological properties of the sample measured under non-oxidative conditions is very small. Within the experimental time of 22000 s (6.1 h), the sample stays within the ±5% limits usually taken as the reproducibility limit of rheology. However, for the sample exposed to oxygen violates these criteria after 330 and 700 s with respect to *G'* and *G"*, respectively. It is interesting to note that *G'* violates the criterion twice as fast as *G"*, which is due to the stronger dependence of *G'* on $M_w$ (Eq. 4) in the terminal regime than *G"* (Eq. 5).

It has to be stated that not all ovens are of the same quality in terms of providing the desired environment (usually non-oxidative for polymer melts and other samples significantly above the room temperature) so that making a comparison of the time of stability of the same sample under the same conditions on different rheometers does not necessarily lead to the same time of stability, as the contamination with oxygen might vary depending on quality of used nitrogen and building quality of the oven.

Furthermore, the sensitivity of a material to thermo-oxidative degradation depends on a variety of factors, ranging from type of polymer (and specific grade) to additives – especially dormant radicals and stabilizers and obviously the measurement temperature. The author has experienced that a PE, which is stable for several days at 150°C, degrades at 210°C within 60 min and at 230°C within 5 min. At 250°C it was not possible anymore to load the sample without finding degradation immediately.

This degradation temperature dependence is obviously material and grade dependent (see also Fig. 14) as is the frequency regime investigated (Fig. 12).

While some materials are hydrophobic – namely polyolefins – many are hydrophilic and, consequently, absorb water from the surroundings. Especially, polycondensates (polyesters and polyamides) absorb up to 12 wt.% $H_2O$, which can lead to rapid depolymerization, when heating the water-containing sample beyond a certain limiting temperature. It should be mentioned that a popular way to produce nanoparticles from organic precursors is hydrothermal synthesis, in which organic precursors and additives are loaded in an autoclave with water and, subsequently, heated to 150-300°C destroying most organic matter (*e.g.* Cheng *et al.*, 2013). Hence, water at high temperatures is capable of degrading many polymers and, thus, should be removed by drying the samples prior to testing the sample at high temperatures.

Furthermore, the water also leads to bubble formation, which was discussed previously.

### 2.2.4. Limit of the linear viscoelastic regime

The determination of the limits of the linear viscoelastic regime is very important to assure that the subsequent tests are conducted in the linear viscoelastic regime. The determination of the limits has to be performed for oscillatory and creep recovery measurements.

Fig. 16 shows a typical data set of an amplitude sweep for the slightly *long-chain branched* sample B7, which is representative for many. It is evident that oscillatory deformations $\gamma_0$ below 0.3% lead to insufficient results because of the small deformation of the sample being at the lower end of the torque resolution of the TA Instruments ARES. At deformations $\gamma_0$ above 30% the onset of the non-linear regime is found. Hence, the tests for this sample should be preferably performed at a deformation $\gamma_0$ around 5%.

Fig. 17 shows the storage compliance of an LCB-mHDPE at different stress levels $\tau_0$. Hence, the deformation is different for each data point. It is clearly observable that under these conditions, a clear deviation is found for $\tau_0 = 10000$ Pa at $\omega = 2.15$ s$^{-1}$, while for $\tau_0 = 1000$ Pa

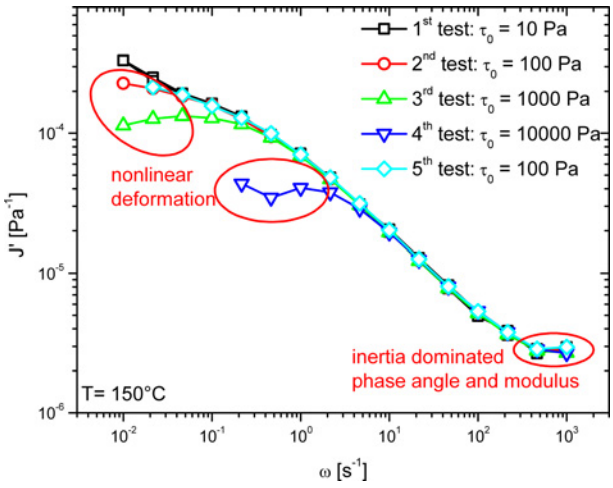


**Fig. 17.** (Color online) Frequency sweep of LCB-mHDPE B5 with different shear amplitudes.

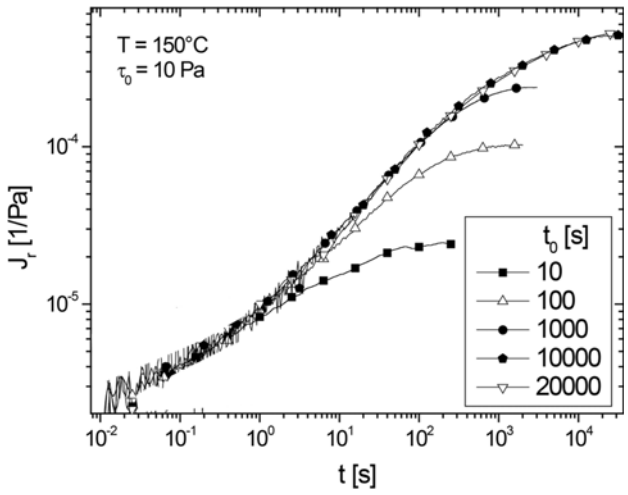


**Fig. 18.** Creep recovery tests of mLLDPE F26F.

at $\omega = 0.215\ s^{-1}$ lead to a deviation from the data acquired at lower $\tau_0$. These two points correspond to a nonlinearity limit $\gamma_0 \approx 100\%$, which is in good agreement of what is typically found for polymer melts and solutions. It should be mentioned that investigations on materials at low $\omega$ or $\dot{\gamma}$ or long times (*i.e.* in creep tests) show a higher nonlinearity limit (Münstedt, 2014, Wolff *et al*., 2010), which, however, is easily explainable by the fact that a Newtonian liquid does not have a linearity limit and in the terminal regime, the material behavior is close to Newtonian, which effectively increases the nonlinearity limit ideally to infinity.

Furthermore, it is obvious from Fig. 17 that the highest frequencies of $\omega = 1000\ s^{-1}$ and to some extent also $\omega = 464\ s^{-1}$ suffer from incorrect phase angles $\delta$, which are caused by the fact that the inertia effect of the geometry scales with $\omega^4$.

### 2.2.5. Sample failure

One of the problems that can be found especially in elongational testing, but which also occurs regularly in shear flows, are various forms of macroscopic and microscopic sample failure (*e.g.* Agassant *et al*., 2006; Münstedt *et al*., 2001; Tapadia and Wang, 2004).

When using high deformations or especially fast shear rates, various forms of wall slip, shear banding or even sample ejection can be observed. Rotational rheometers are more sensitive to these problems than capillary rheometers due to their open geometry and limited sample volume (not a continuous flow but the same sample is measured over and over again), which allows defects to propagate. Usually, such sample failures only occur under conditions far in the nonlinear regime, which is far less understood than the linear viscoelastic regime.

When having rather low viscous materials and shearing them with high shear rates, it can also happen that the centrifugal forces become larger than the cohesive strength of the sample, which leads to ejection of the sample out of the geometry. This type of sample failure is very easy to detect after the experiment, because some of the same is found on the wall of the oven and a significant fraction of the geometry is empty.

Methods against this way of failure are to either use a Couette geometry or to use a cone with a small angle or a parallel plate with a small gap – the last two preferably with a smaller plate diameter. The last two methods will decrease the gap at the outer end of the geometry and, consequently, increase the capillary forces working against ejection. Furthermore, as shown in Eq. 1 for parallel plates and in

$$\dot{\gamma} = \Omega/\beta \tag{7}$$

with β - cone angle for cone and plate geometries, reducing gap and cone angle, respectively, reduces the rotational speed Ω of the geometry and, thus, the centrifugal forces. However, small cone angles or gaps make a measurement much more susceptible to geometry imperfections, which means that only very good geometries can be taken for such critical measurements.

Furthermore, samples, which are low enough in viscosity to show a tendency to be ejected, might also have a tendency to evaporate, which, for example, was observed by the author for higher alkenes (heptadecane, hexacosene) at 150°C. However, this could be easily detected by a distinct waxy smell of the sample in the laboratory.

Significant literature has been published on this topic (*e.g.* Agassant *et al*., 2006; Münstedt *et al*., 2001; Tapadia and Wang, 2004), which will not be discussed in more detail here.

## 3. Conclusions

Rheometry has gained an important place in polymer science, chemical engineering, biomedical science and engineering, and related disciplines, but the fact that the number of users expands due to the apparent ease of using modern test setups, many inexperienced users obtain data, which is significantly error afflicted in nontrivial ways.

The article described some typical problems we encounter when measuring molten polymers. While most of the possible rheometer artefacts are encountered for other systems (*e.g.* polymer blends, composites, solutions, gels, …) as well, the material related artefacts are polymer specific.

When following a check list of the possible artefacts outlined in the article, unexperienced readers should be able to avoid many of the potential issues presented. In this respect, the author hopes that this article will contribute to an improvement of the quality of rheological data published.

## Acknowledgments

The author would like to acknowledge the many funding agencies, which funded the author's research in the past 14 years, in which among many correct results these faulty results were collected: Deutsche Forschungsgemeinschaft, "Actions de Recherches Concertées" of the Communauté Française de Belgique, and National Research Foundation of Korea (grant: 110100713). The author would also like to thank Prof. Dr. H. Münstedt (FAU Erlangen-Nürnberg), Prof. Dr. C. Bailly (Univ. catholique de Louvain), Prof. Dr. C.-Y. Liu (Chinese Academy of Science), Prof. Dr. J. Dealy (McGill Univ.), Dr. J. Kaschta (FAU Erlangen-Nürnberg), and Dr. Aly Franck (TA Instruments) for many discussions about experimental challenges on rheometry.

## References

Agassant, J.F., D.R. Arda , C. Combeaud, A. Merten, H. Munstedt, M.R. Mackley, L. Robert, and B. Vergnes, 2006, Polymer processing extrusion instabilities and methods for their elimination or minimisation, *Int. Polym. Proc.* **21**, 239-255.

Auhl, D., 2006, *Molekulare struktur und rheologische eigenschaften von strahlenmodifizierten polypropylen*, Lehrstuhl für Polymerwerkstoffe, Erlangen, Friedrich-Alexander Universität Erlangen-Nürnberg, Ph. D.

Barnes, H.A., and D. Bell, 2003, Controlled-stress rotational rheometry: An historical review, *Korea-Aust. Rheol. J.* **15**, 187-196.

basell Polyolefins, 2003, *Polyethylen - Produkte und eigenschaften*.

Cheng, G., M.S. Akhtar, O.B. Yang, and F.J. Stadler, 2013, Novel preparation of anatase TiO2@reduced graphene oxide hybrids for high-performance dye-sensitized solar cells, *ACS Appl. Mater. Interfaces* **5**, 6635-42.

Dealy, J., R.G. Larson, 2006, *Structure and rheology of molten polymers - From structure to flow behavior and back again*, Munich, Hanser.

den Doelder, J., 2004, Personal communication (eMail).

Dijkstra, D.J., 2009, Guidelines for rheological characterization of polyamide melts, *Pure Appl. Chem.* **81**, 339-349.

Edler, R., 1986, *Aufbau eines rheometers mit magnetischer lagerung*, Lehrstuhl für Kunststoffe, Erlangen, Friedrich-Alexander University Erlangen-Nürnberg, Diploma.

Friedrich, C., and Y.Y. Antonov, 2007, Interfacial relaxation in polymer blends and gibbs elasticity, *Macromolecules* **40**, 1283-1289.

Frischknecht, A.L., S.T. Milner, A. Pryke, R.N. Young, R. Hawkins, and T.C.B. McLeish, 2002, Rheology of three-arm asymmetric star polymer melts, *Macromolecules* **35**, 4801-4820.

Gabriel, C., and J. Kaschta, 1998, Comparison of different shear rheometers with regard to creep and creep recovery measurements, *Rheol. Acta* **37**, 358-364.

Gabriel, C., and H. Münstedt, 1999, Creep recovery behavior of metallocene linear low-density polyethylenes, *Rheol. Acta* **38**, 393-403.

Gabriel, C., 2001, *Einfluss der molekularen Struktur auf das viskoelastische Verhalten von Polyethylenschmelzen*, Aachen, Shaker-Verlag.

Graessley, W.W., 2008, *Polymeric liquids & networks: Dynamics and rheology*, London, Taylor & Francis.

Kaminsky, W., 2004, Personal Communication.

Karimkhani, V, T.F. Afshar, S. Pourmahdian, and F.J. Stadler, 2013, Revisiting long-chain branch formation mechanism in metallocene catalyzed polyethylenes, *Polym. Chem.* **4**, 3774-3790.

Klimke, K., 2006, *Optimised polyolefin branch quantification by $^{13}C$ NMR spectroscopy*, Mainz, Max-Planck Institute of Polymers, Ph.D.

Link, G., and F.R. Schwarzl, 1985, Measuring device for precise evaluation of torsional creep and recovery data, *Rheol. Acta* **24**, 211-219.

Liu, C.Y., M.L. Yao, R.G. Garritano, A.J. Franck, and C. Bailly, 2011, Instrument compliance effects revisited: linear viscoelastic measurements, *Rheol. Acta* **50**, 537-546.

McLeish, T.C.B., J. Allgaier, D.K. Bick, G. Bishko, P. Biswas, R. Blackwell, B. Blottiere, N. Clarke, B. Gibbs, D.J. Groves, A. Hakiki, R.K. Heenan, J.M. Johnson, R. Kant, D.J. Read, and R.N. Young, 1999, Dynamics of entangled H-polymers: Theory, rheology, and neutron-scattering, *Macromolecules* **32**, 6734-6758.

Münstedt, H., M. Schwetz, M. Heindl, and M. Schmidt, 2001, Influence of molecular structure on secondary flow of polyolefin melts as investigated by laser-Doppler velocimetry, *Rheol. Acta* **40**, 384-394.

Münstedt, H., T. Steffl, and A. Malmberg, 2005, Correlation between rheological behaviour in uniaxial elongation and film blowing properties of various polyethylenes, *Rheol. Acta* **45**, 14-22.

Münstedt, H., 2014, Rheological experiments at constant stress as

efficient method to characterize polymeric materials, *J. Rheol.* **58**, 565-587.

Ngai, K.L., and D.J. Plazek, 2007, Temperature dependences of the viscoelastic response of polymer systems, In: J.E. Mark ed., *Physical properties of polymers handbook*, Heidelberg, Springer.

Patham, B., and K. Jayaraman, 2005, Creep recovery of random ethylene-octene copolymer melts with varying comonomer content, *J. Rheol.* **49**, 989-999.

Piel, C., 2004, Personal communication.

Piel, C, F.J. Stadler, J. Kaschta, S. Rulhoff, H. Münstedt, and W. Kaminsky, 2006a, Structure-property relationships of linear and long-chain branched metallocene high-density polyethylenes characterized by shear rheology and SEC-MALLS, *Macromol. Chem. Physic.* **207**, 26-38.

Piel, C, P. Starck, J.V. Seppälä, and W. Kaminsky, 2006b, Thermal and mechanical analysis of metallocene-catalyzed ethene–α-olefin copolymers: The influence of the length and number of the crystallizing side chains, *J. Polym. Sci. Pol. Chem.* **44**, 1600-1612.

Plazek, D.J., 1968, Magnetic Bearing Torsional Creep Apparatus, *J. Polym. Sci. Pol. Phys.* **6**, 621-638.

Rulhoff, S., and W. Kaminsky, 2006, Direct copolymerization of propene and ethene-based macromers to produce long chain branched syndiotactic polypropene, *Macromol. Symp.* **236**, 161-167.

Stadler, F.J., C. Piel, K. Klimke, J. Kaschta, M. Parkinson, M. Wilhelm, W. Kaminsky, and H. Münstedt, 2006a, Influence of type and content of various comonomers on long-chain branching of ethene/α-olefin copolymers, *Macromolecules* **39**, 1474-1482.

Stadler, F.J., C. Piel, W. Kaminsky, and H. Münstedt, 2006b, Rheological characterization of long-chain branched polyethylenes and comparison with classical analytical methods, *Macromol. Symp.* **236**, 209-218.

Stadler, F.J., C. Piel, J. Kaschta, S. Rulhoff, W. Kaminsky, and H. Münstedt, 2006c, Dependence of the zero shear-rate viscosity and the viscosity function of linear high-density polyethylenes on the mass-average molar mass and polydispersity, *Rheol. Acta* **45**, 755-764.

Stadler, F.J., C. Gabriel, and H. Münstedt, 2007, Influence of short-chain branching of polyethylenes on the temperature dependence of rheological properties in shear, *Macromol. Chem. Physic.* **208**, 2449-2454.

Stadler, F.J., and H. Münstedt, 2008, Terminal viscous and elastic properties of linear ethene/α-olefin copolymers, *J. Rheol.* **52**, 697.

Stadler, F.J., J.-M. Schumers, C.-A. Fustin, J.-F. Gohy, W. Pyckhout-Hintzen, and C. Bailly, 2009, Linear viscoelastic rheology of moderately entangled telechelic polybutadiene temporary networks, *Macromolecules* **42**, 6181-6192.

Stadler, F.J., B. Arikan, J. Kaschta, and W. Kaminsky, 2010, Long-chain branches in syndiotactic polypropene induced by vinyl chloride, *Macromol. Chem. Physic.* **211**, 1472-1481.

Stadler, F.J., V. Karimkhani, 2011, Correlations between the characteristic rheological quantities and molecular structure of long-chain branched metallocene catalyzed polyethylenes, *Macromolecules* **44**, 5401-5413.

Tao, F.F., D. Auhl, A.C. Baudouin, F.J. Stadler, and C. Bailly, 2013, Influence of multiwall carbon nanotubes trapped at the interface of an immiscible polymer blend on interfacial tension, *Macromol. Chem. Physic.* **214**, 350-360.

Tapadia, P., and S.Q. Wang, 2004, Nonlinear flow behavior of entangled polymer solutions: Yieldlike entanglement-disentanglement transition, *Macromolecules* **37**, 9083-9095.

Walter, P., S. Trinkle, D. Lilge, C. Friedrich, and R. Mulhaupt, 2001, Long chain branched polypropene prepared by means of propene copolymerization with 1,7-octadiene using MAO-activated rac-Me2Si(2-Me-4-phenyl-Ind)(2)ZrCl2, *Macromol. Mater. Eng.* **286**, 309-315.

Wilhelm, M., 2002, Fourier-transform rheology, *Macromol. Mater. Eng.* **287**, 83-105.

Williams, M.L., R.F. Landel, and J.D. Ferry, 1955, The temperature dependence of relaxation mechanisms in amorphous polymers and other glass-forming liquids, *J. Am. Chem. Soc.* **77**, 3701-3707.

Wolff, F., J.A. Resch, J. Kaschta, and H. Münstedt, 2010, Comparison of viscous and elastic properties of polyolefin melts in shear and elongation, *Rheol. Acta* **49**, 95-103.

Wolff, F., and H. Münstedt, 2013, Artefacts of the storage modulus due to bubbles in polymeric fluids, *Rheol. Acta* **52**, 287-289.